

SHALLOW LUNAR SEISMIC ACTIVITY AND THE CURRENT STRESS STATE OF THE MOON. T. R. Watters¹, R. C. Weber², G. C. Collins³, and C. L. Johnson^{4,5}. ¹Center for Earth and Planetary Studies, National Air and Space Museum, Smithsonian Institution, Washington, DC 20560, USA (watterst@si.edu); ²NASA Marshall Space Flight Center, Huntsville, AL 35805, USA; ³Physics and Astronomy Department, Wheaton College, Norton, MA 02766, USA; ⁴Dept. of Earth, Ocean and Atmospheric Sciences, University of British Columbia, Vancouver, British Columbia, V6T 1Z4, Canada; ⁵Planetary Science Institute, Tucson, AZ 85719, USA.

Introduction: A vast, global network of more than 3200 lobate thrust fault scarps has been revealed in high resolution Lunar Reconnaissance Orbiter Camera (LROC) images [1-6]. The fault scarps very young, <50 Ma, based on their small scale and crisp appearance, crosscutting relations with small-diameter impact craters, and rates of infilling of associated small, shallow graben and may be actively forming today [1-3].

The population of young thrust fault scarps provides a window into the recent stress state of the Moon and offers insight into the origin of global lunar stresses. The distribution of orientations of the fault scarps is non-random, inconsistent with isotropic stresses from late-stage global contraction as the sole source of stress. Modeling shows that tidal stresses contribute significantly to the current stress state of the lunar crust [1]. Tidal stresses (orbital recession and diurnal tides) superimposed on stresses from global contraction result in non-isotropic compressional stress and thrust faults consistent with lobate scarp orientations. Stresses due to orbital recession do not change with orbital position, thus it is with the addition of diurnal stresses that peak stresses are reached. At apogee, diurnal and recession stresses are most compressive near the tidal axis, while at perigee they are most compressive 90° away from the tidal axis [7]. Coseismic slip events on currently active thrust faults are expected to be triggered when peak stresses are reached. Analysis of the timing of the 28 the shallow moonquakes recorded by the Apollo seismic network shows that 19 indeed occur when the Moon is closer to apogee, while only 9 shallow events occur when the Moon is closer to perigee [7]. Here we show the results of relocating the shallow moonquake using an algorithm designed for sparse networks [12] to better constrain their epicentral locations in order to compare them with stress models. The model for the current stress state of the Moon is refined by investigating the contribution of polar wander.

Current Stress State and Polar Wander: Radial contraction from interior cooling is the dominant source of stress, contributing ≥ 2 but <10 MPa based on the currently mapped population of lobate scarps [1, 2]. Superimposed on compressional stresses from contraction σ_c are two components of tidal stress, orbital recession stress σ_r and diurnal stress σ_d . Tidal stresses are dominated by σ_r that may reach 20 to 40 kPa [1]. An additional component of stress that may significantly con-

tribute to the current lunar stress state is polar wander. True polar wander has been attributed to a change in the Moon's moments of inertia due to a low-density thermal anomaly beneath Procellarum [8]. The change in the location of the poles is consistent with the observed remnant polar hydrogen deposits [8]. Modeling shows that stresses from $\sim 3^\circ$ of polar wander σ_w over the last 1 billion years results in stresses with orientations and magnitudes similar to σ_r (Fig. 2). The net non-isotropic compressional stresses σ_n from $\sigma_r + \sigma_w + \sigma_c$ result in thrust faults with preferred orientations that are in general agreement with orientations of the mapped faults (Fig. 3). Although the contribution of diurnal tidal stresses to σ_n is small (≤ 5 kPa), the addition of σ_d results in peak stress when the Moon is near apogee or perigee, consistent with the occurrence of most shallow seismic events [7].

Shallow Moonquakes: Four seismometers were placed on the Moon at the Apollo 12, 14, 15 and 16 landing sites. During the operation of the seismometers (1969 to 1977), 28 shallow moonquakes were recorded [9, 10] (Fig. 1). Shallow moonquakes occur at depths <200 km and have been interpreted as tectonic in origin [10]. Analysis of all 28 shallow moonquakes indicates Richter-equivalent magnitudes in the range from 1.6 to 4.2 [10]. Estimates of stress drops range from a few MPa to over 100 MPa for the 3 largest events [11].

The current best estimates for most shallow moonquake locations are likely only accurate to several degrees, possibly more for small and/or distant events. This makes a comparison with stress models and attempts to match the exact locations of known tectonic features with specific shallow moonquakes problematic. Their depths are similarly ill-constrained, with some estimated to occur at the surface, and others up to 200 km deep with uncertainty up to an additional 200 km.

The standard method for locating a seismic event uses a known velocity model and the observed arrival times of the direct P and S waves. Large uncertainties in arrival times directly translate into a large uncertainty in event location. We have instead applied a location algorithm specifically designed for sparse networks [12] to determine whether their location accuracy can be improved. Rather than solving for a best-fit location, this approach divides the solution set into falsified and non-falsified candidate locations using an adaptive grid search, and accounts for arrival time uncertainty using

windows around the true arrival time. Preliminary results suggest that as many as half of the published shallow moonquake locations may fall outside the non-falsified regions.

References: [1] Watters T.R. et al. (2015) *Geology*, 43, 851–854. [2] Watters T.R. et al. (2010) *Science*, 329, 936-940. [3] Watters, T.R. et al. (2012) *Nature Geoscience*, doi:10.1038/NGEO1387. [4] Watters T.R. and Johnson C.L. (2010) in *Planetary Tectonics*, Cambridge

Univ. Press, pp. 121-182. [5] Banks, M. E. et al. (2012) *J. Geophys. Res.*, 117, doi:10.1029/2011JE003907. [6] Williams, N.R. et al. (2013) *J. Geophys. Res.*, doi: 10.1002/jgre.20051. [7] Watters, T.R. et al. (2016) *LPSC 47*, #1642. [8] Siegler, M.A. et al. (2016) *Nature* 531, 480-484. [9] Nakamura, Y. et al. (1981) *Tech. Rep. 118*, Inst. for Geophys., Univ. of Tex. Austin. [10] Nakamura, Y. et al. (1979) *Proc. Lunar Sci. Conf.* 10, 2299-2309. [11] Oberst, J. (1987) *J. Geophys. Res.*, 92, 1397-1405. [12] Knapmeyer, M. (2008) *Geophys. J. Int.* 175, 975-991.

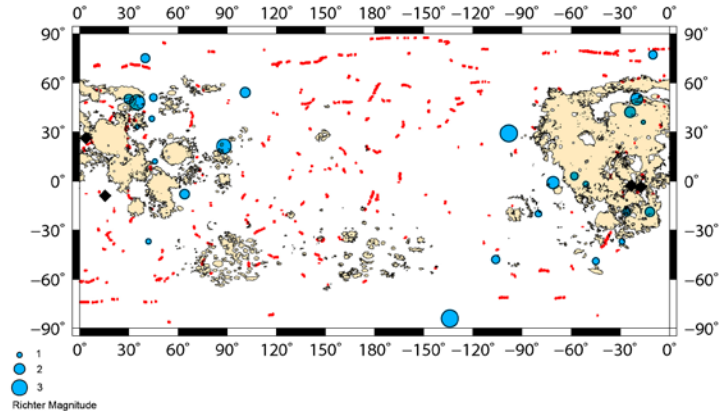


Figure 1. Map of lobate scarps (red), epicentral locations of shallow moonquakes (blue dots), and locations of Apollo Seismic Network seismometers (black diamonds). Moonquakes are scaled by estimated Richter magnitude [10]. Mare basalt units are shown in tan.

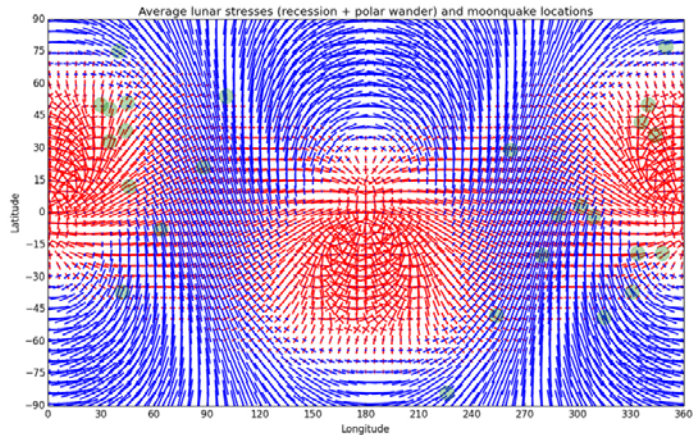


Figure 2. Orientations of principal stresses due to orbital recession and polar wander. Compressional stress components are show by red lines and reach a maximum of ?? kPa. Extensional stress components are shown by blue lines.

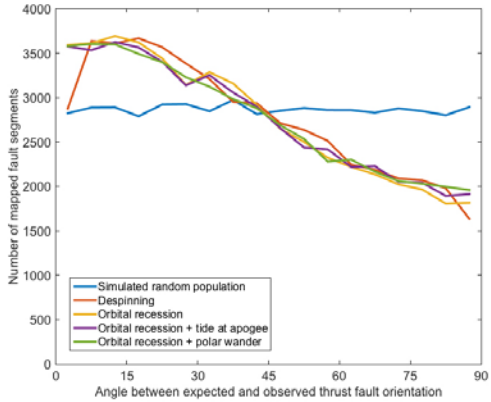


Figure 3. Agreement between observed faults and expected local thrust fault orientations due to different stress models. Fault segments at 0 on plot are orthogonal to local direction of most compressive stress, and at 90 they are parallel to most compressive stress.